Evaluation of Nonconventional Additives as Fire Retardants on Polyamide 6,6: Phosphorous-Based Master Batch, α-Zirconium Dihydrogen Phosphate, and β-Cyclodextrin Based Nanosponges

Daniela Enescu, Jenny Alongi, Alberto Frache

Dipartimento di Scienza dei Materiali e Ingegneria Chimica, Politecnico di Torino, Alessandria Branch, Viale T. Michel, 5, 15121 Alessandria, Italy

Received 24 February 2011; accepted 7 May 2011
DOI 10.1002/app.34874
Published online 20 September 2011 in Wiley Online Library (wileyonlinelibrary.com).

ABSTRACT: The influence of new types of additives, such as halogen- and antimony-free flame-retardant master batches based on phosphorus, α-zirconium dihydrogen phosphate, and β-cyclodextrin nanosponges, on the flame retardancy of polyamide 6,6 (PA6,6) by means of cone calorimetry and limiting oxygen index (LOI) tests was investigated. A significant decrease of the heat release rate, depending by the type of additive used, was observed. Furthermore, with the consideration that the life safety during the fire could be improved by a decrease in the fire hazard, a decrease in the quantity of the smoke and its toxicity, depending also on the type of additive, was revealed. With regard to the LOI test, neat PA6,6 showed a slight increase in the LOI value in comparison with the PA6,6 composites. However, all of the PA6,6/composites showed a slower burning velocity and antidripping effects at oxygen concentrations corresponding to the LOI value. To understand the flame-retardancy mechanism of these novel PA6,6 composites, we thoroughly investigated their thermal decomposition behavior and microstructure/elemental analysis by scanning electron microscopy/energy-dispersive X-ray spectroscopy. Furthermore, the combustion behavior of these novel PA6,6 composites was compared with that of conventional nanofillers (e.g., modified montmorillonite clay and carbon nanotubes). © 2011 Wiley Periodicals, Inc. J Appl Polym Sci 123: 3545–3555, 2012

Key words: composites; flame retardance; thermal properties

INTRODUCTION

Thanks to its superior intrinsic properties, such as resistance to chemicals, fatigue, abrasion, and creep, low friction, high tensile strength and melting point, and good processability, polyamide 6,6 (PA6,6) remains as one thermoplastic of great importance in the industrial sector.

To improve PA6,6's properties, some studies on its flame retardancy have been carried out, and it has been demonstrated that the use of halogen-free flame retardants[1–7] and, more recently, nanofillers[8,9] can be an ecofriendly alternative to the use of halogen-based flame retardants, which despite their remarkable fire resistance,[10–15] show serious drawbacks during burning, such as the emission of corrosive and toxic halogen compounds and obscuring smoke.[16–19]

For example, Schartel et al.[2] investigated the influence of red phosphorus (RP) on the fire retardancy of glass-fiber (GF) reinforced PA6,6. The fire tests showed that PA6,6-GF/RP was an effective charring material, achieving a remarkable reduction in terms of the heat release rate and total heat involved in cone calorimeter tests and the highest self-extinction classification V-0 in UL 94 tests, whereas in the case of PA6,6–GF, all of the polymeric material was consumed so that only the GFs remained.

Gijsman et al.[3] studied the influence of melamine cyanurate (MC) as a halogen-free flame retardant on PA6,6. They suggested that the degradation products formed in PA6,6 (cyclopentanone) may have cross-linked with MC degradation products (mainly NH_3), which resulted in less flammable high-molecular-weight structures. Later, Liu and Wang[4] reported that the addition of MC–microencapsulated RP into PA6,6 led to a satisfactory fire retardancy. They proposed that the mechanism of fire retardancy was based on a nitrogen–phosphorus synergistic effect between MC and RP.

As far as the effect of conventional nanofillers (i.e., montmorillonite) on the fire retardancy of PA6,6 is concerned, Qin et al.[8] showed that with the nanofiller presence, a ceramic-like char formed on the surface of nanocomposites during burning; this insulated the underlying material and slowed the mass loss rate of the decomposition products.

Correspondence to: D. Enescu (daniela.enescu@polito.it).

Song et al.[9] examined the combination of modified montmorillonite clay with MC. The results show that the combination of the nanofiller with the MC led to a remarkable reduction in the heat release rate peak of the nanocomposite ($\leq$64%) compared with that of neat PA6,6. The enhanced flame-retardant properties of the nanocomposites compared with neat PA6,6 was attributed to the ceramic-like char formation and the synergistic effect between the nanoscale clay layers and MC.

With the aim of extending the range of ecofriendly flame retardants, in this study, we investigated the influence of new types of additives on the fire retardancy of PA6,6. Furthermore, the fire behavior of these new additives was compared with that of conventional nanofillers (modified montmorillonite clay and carbon nanotubes).

EXPERIMENTAL

Materials

The PA6,6 used was a commercial-grade product supplied by Rhodia (Paris, France) in pellet form. CESAflam ABA0050162 (CESA) was a master batch based on polyamide 6 and a halogen- and antimony-free flame retardant based on phosphorus supplied by Clariant (Milan, Italy) in pellet form. α-Zirconium dihydrogen phosphate [α—$Zr(HPO_4)_2 \cdot H_2O$ (ZrP)], supplied by Rhodia (Paris, France) in aqueous suspension form, was dried on a heating plate at 80°C for at least 4 days. The resulting powder was further dried in a vacuum oven at 80°C for 12 h. β-Cyclodextrin-based nanosponges (NSs) represent a class of cyclic oligosaccharides with cavities a few nanometers wide. The NSs used in this work were based on β-cyclodextrin (cyclic oligosaccharide formed by six to eight glucose molecules bonded with a 1,4-α glucosidic bond and having a characteristic truncated cone structure) and were prepared according to a procedure described previously.[20] Cloisite 30 B (C30B) was a natural montmorillonite clay modified with methyl, tallow, bis-2-hydroxyethyl quaternary ammonium chloride supplied by Southern Clay Products, Inc., (Austin, Texas , USA) in powder form. Plasticyl PA 1501 was a master batch based on PA6,6 and 15 wt % multiwall carbon nanotubes (MBCNTs) supplied by Nanocyl (Sambreville , Belgium) in pellet form. Before use, all of the products were dried in a vacuum oven at 80°C for 6 h and another 6 h only *in vacuo* before use.

Sample preparation

All of the PA6,6 composites (PA6,6/10 wt % CESA, PA6,6/10 wt % ZrP, PA6,6/5 wt % C30B, and PA6,6/2 wt % MBCNTs), with the exception of the PA6,6/10 wt % NS composite, were prepared via direct melt compounding with a Leistritz ZSE 18 HP (Brabender Technologie, Duisburg, Germany) corotating twin screw extruder [screw diameter = 18 mm, length/diameter = 40]. The operating temperature of the extruder was maintained at 270–270–265–260–260–260–260–260°C from the hopper to the die, respectively. The screw speed was maintained at 150 rpm, and the throughput was 4.5 kg/h. The molten material was quenched in water and then pelletized. The PA6,6/10 wt % NS composite was prepared with an internal Rheomix-Brabender OHG 47055 (Belotti Strumenti Srl, Milan, Italy) mixer, and the screw speed was kept constant at 50 rpm for 2 min at 260°C under a nitrogen flow to prevent the oxidation of PA6,6. The pellets were dried in a vacuum oven at 80°C for 6 h and another 6 h only *in vacuo* before use.

Measurements

Morphology

Scanning electron microscopy (SEM)/energy-dispersive X-ray spectroscopy (EDS). The microstructural and elemental analyses of the samples were done with a scanning electron microscope (LEO 1450 VP, Oberkochen , Germay) with an energy-dispersive X-ray probe (INCA Energy Oxford, UK) attachment. The cross-sectional samples were prepared by cryogenic fracture in liquid nitrogen and then sputter-coated with gold for 27 s at a working pressure of 0.1 mbar before the SEM/EDS measurements to increase their electrical conductivity to prevent the accumulation of a static electric charge on the specimen during electron irradiation and to enhance the surface detail.

Thermal analysis

Thermogravimetric (TG) analyses were performed with a Q 500 thermal analyzer (TA Instruments, Chicago, Illinois , USA) at a heating rate of 10°C/min from 50 to 800°C under a nitrogen flow (40 mL/min) and in isothermal conditions at 390°C for 120 min under a nitrogen flow. The samples (ca. 10 mg) were placed in open alumina pans. From TG curves, the parameters T_{onset} (the temperature at which the sample lost 5 wt % of its original mass) and T_{max} (the temperature at which the maximum rate of mass loss occurred) were evaluated to characterize the thermal stability of the neat additives and composites.

To determine the existence of interaction between the compounds of the PA6,6 composites, the experimental TG curves of the PA6,6 composites were compared with the calculated TG curves. The calculated mass loss (M_{th}) curves were calculated by the linear combination of the experimental TG curves of each compound taken individually (PA6,6 and additives):

$$M_{th}(T) = xM_{PA6,6}(T) + yM_{additive}(T)$$

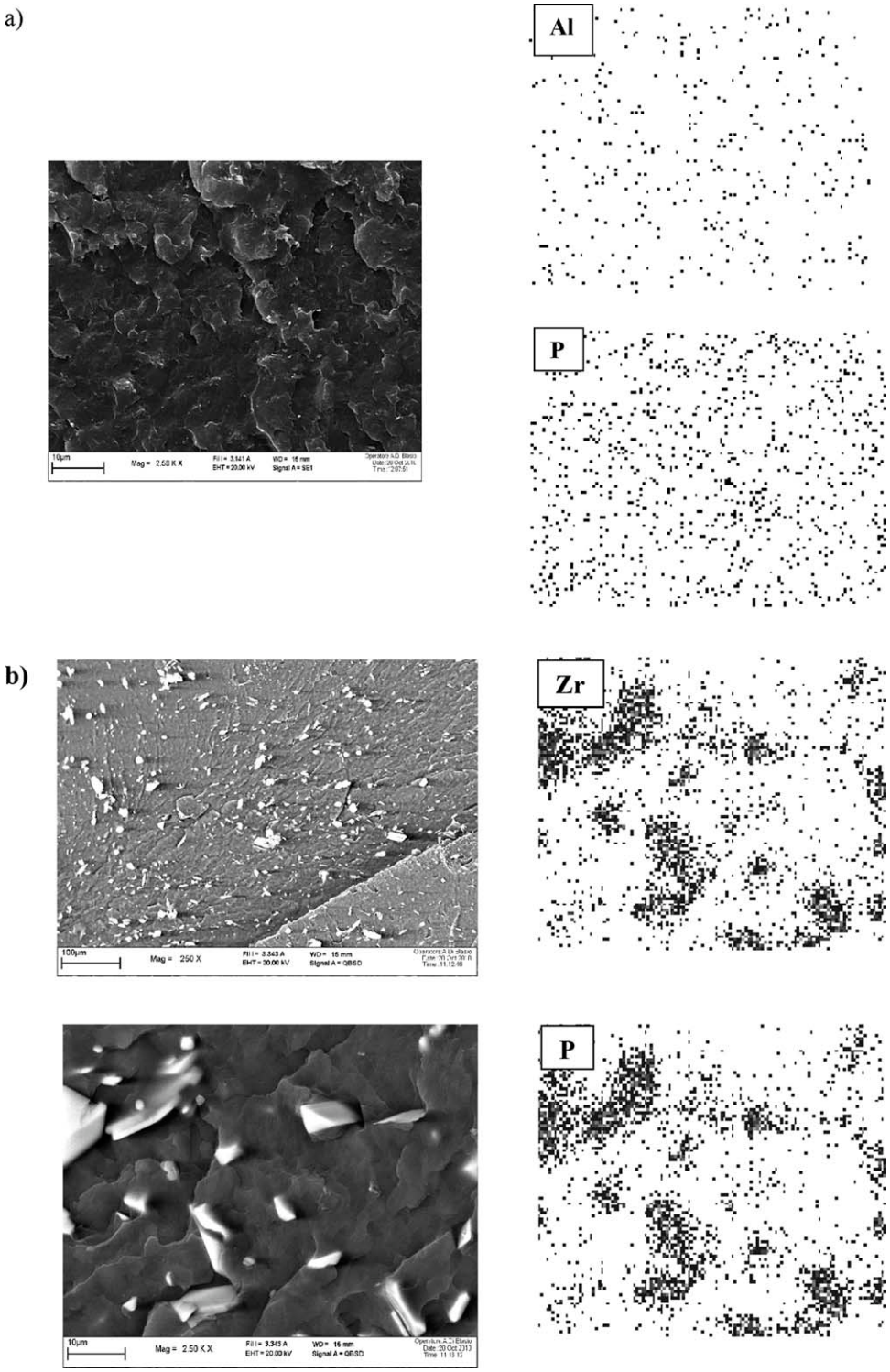

Figure 1 SEM micrograph and elemental distribution from EDS mapping of the (a) PA6,6/CESA, (b) PA6,6/ZrP, and (c) PA6,6/NS composites.

where $M_{PA6,6}$ is the mass loss of PA6,6, $M_{additive}$ is the mass loss of additive and T is the temperature of degradation (50–800 °C) $x + y = 1$ and x and y are the mass percentages of PA6,6 and additive in the composite. In other words, the calculated curves, calculated by additives rules, represent the degradation of the composite when no chemical or physical interaction between the compounds takes place.

Fire tests. The limiting oxygen index (LOI) test was carried out with a Fire Testing Laboratories (Fire Instrumentation & Research Equipment Ltd , Kent, UK) instrument according to the standard oxygen

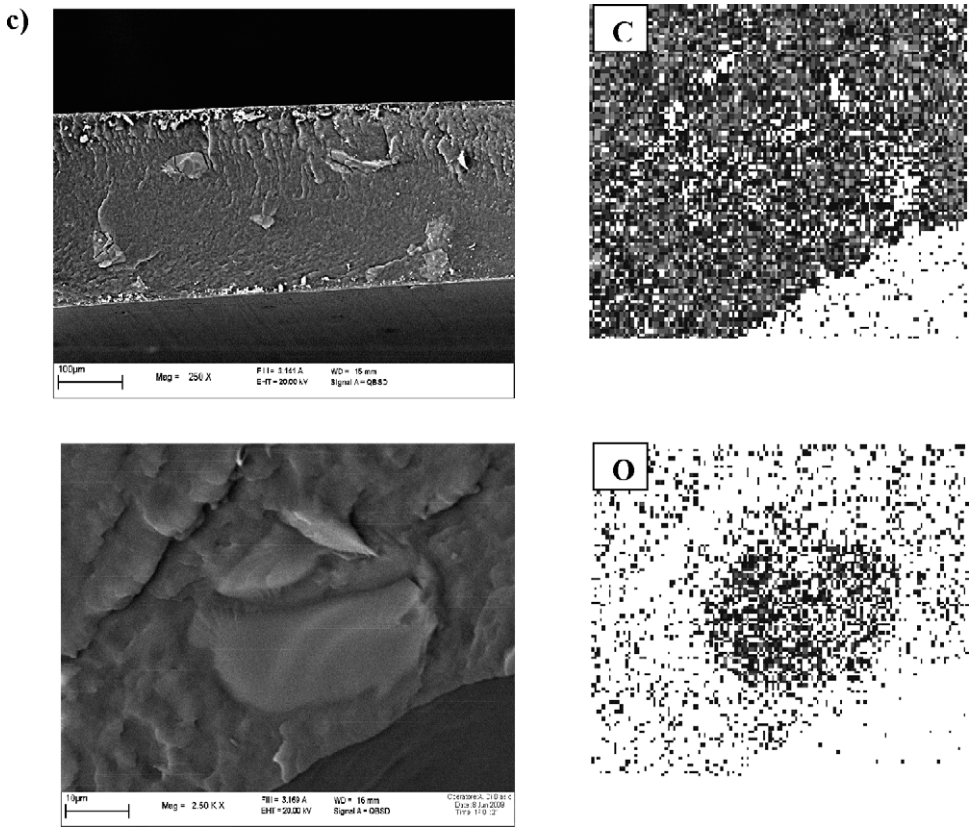

Figure 1 (Continued)

index test UNI EN ISO 4589-2. This test is a procedure for measuring the minimum concentration of oxygen in a flowing mixture of oxygen and nitrogen that supports combustion in a candlelike configuration of a top-ignited vertical test specimens.

Cone calorimetry testing was carried out in accordance with the ISO-5660-1 standard procedure with a Fire Testing Technology cone calorimeter (East Greenstead, UK). The bottom and the sides of each specimen, prepared by compression molding in a laboratory press equipped with heating plates (GiBitre Instruments, Bergamo, Italy) at 260°C, were wrapped in an aluminum foil and exposed horizontally to an external heat flux of 35 kW/m^2, the recommended value for heat flux for initial studies to mimic small-scale fires.[21] The main parameters measured were time to ignition (TTI; s), peak heat release rate (PHRR), which is proportional to the maximum intensity reached by a fire (kW/m^2), total smoke release (TSR, m^2/m^2), evolution of carbon monoxide (CO; ppm), and fire grow rate index (FIGRA; kW·m^{-2}·s^{-1}). FIGRA, a parameter defined as the ration of PHRR/time to PHRR, is an index for estimating fire growth.[22] For each composition, a total of three specimens were tested to ensure significant and reproducible data. The average value and its standard deviation (σ) is reported. The dimensions of the specimens were 50 × 50 × 3 mm^3.

RESULTS AND DISCUSSION

State of additive dispersion into the PA6,6 composites

The SEM micrograph of the PA6,6/CESA composite [Fig. 1(a)] indicated a quite uniform nanometric dispersion of the additive within the PA6,6 matrix; no aggregates of micronic size were visible. Furthermore, EDS mapping revealed that the P and Al elements (black spots) were homogeneously distributed within the PA6,6 matrix (light area).

In contrast, SEM/EDS analysis of the PA6,6/ZrP [Fig. 1(b)] and PA6,6/NS composites [Fig. 1(c)] revealed the existence of aggregates distributed all over the matrix (with some of them having diameters of up to 10 and 35 μm for ZrP and NS, respectively).

Thermal stability

TG analysis can be an useful technique, not only to describe the thermal decomposition process and the effects of additives on a polymer matrix's thermal performance but also to investigated the chemical reactivity of the additive with the polymer matrix by a comparison of the experimental degradation curve with the calculated one.

Figure 2 shows the TG and differential TG curves of neat PA6,6, CESA, ZrP, and NS.

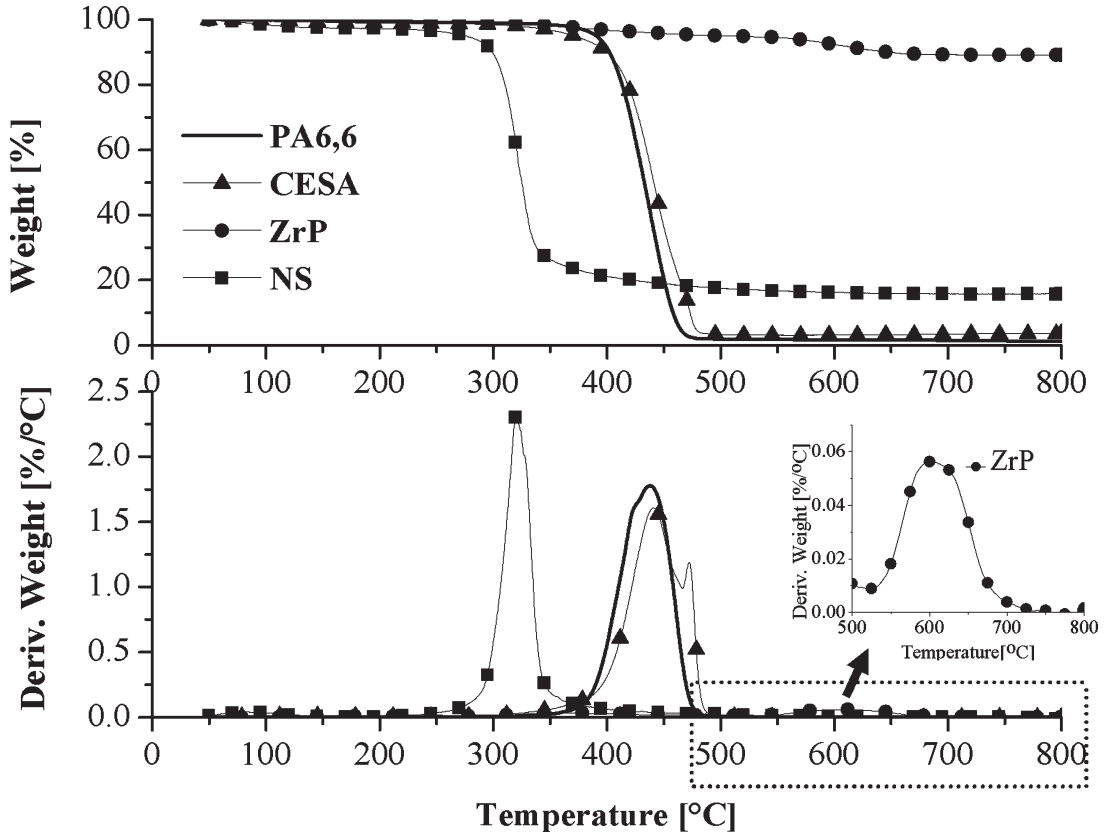

Figure 2 TG curves of neat PA6,6, CESA, ZrP, and NS.

Neat PA6,6 decomposed in one step with T_{max} at 438°C and gave a small solid residue at the end of the test, about 1 wt %. According to the literature,[3,23–25] the major product observed in the degradation of PA6,6 is cyclopentanone, but also present are some hydrocarbons, nitriles, vinyl fragments, CO, carbon dioxide, ammonia, and water.

The degradation of CESA occurred in one major step, with T_{max} at 441°C, followed by a second minor loss with T_{max} at 473°C, and gave 4 wt % of solid residue at 800°C. The CESA residue obtained at 800°C was investigated by SEM/EDS analysis, and this revealed the presence of the aluminum and phosphorous elements (data not shown).

For ZrP, three distinct steps of degradation, with T_{max} values at 163, 363, and 603°C, respectively, were found, which belonged to the loss of crystallization water and also to the condensation of the hydroxyl groups of the phosphate group, leading, in this way, to the formation of zirconium pyrophosphate.[26–29] The residue at the end of the test was 89 wt %.

The degradation of NS occurred in one step with T_{max} at 321°C, leaving a thermal stabile carbonaceous residue at 800°C of 16 wt %. According to Trotta et al.,[30] it is assumed that the degradation process of NS involves the loss of the glucosidic structure and hydroxyl groups; this leads to the formation of unsaturation, carbonyl groups, and aromatic structures.

Table I and Figure 3(a–c) show the TG experimental and calculated curves of the PA6,6/CESA, PA6,6/ZrP, and PA6,6/NS composites.

The addition of CESA into PA6,6 led to a decrease in the temperature of degradation (with the beginning of the degradation at 366°C instead of 391°C for neat PA6,6, and T_{max} at 415°C instead of 438°C). However, a small stabilization of the PA6,6/CESA composite was observed at high temperatures (from 466 to 482°C). In contrast, the addition of ZrP into PA6,6 led to increases of T_{onset} by 6°C and T_{max} from 438°C in PA6,6 to 452°C in the PA6,6/ZrP composite.

As far as the addition of NS into PA6,6 was concerned, a significant decrease of T_{onset} of the PA6,6/NS composite was seen (ca. 53°C);

TABLE I
Thermal Behavior of the Neat PA6,6 and the PA6,6 Composites

Formulation	T_{onset} (°C)	T_{max} (°C)	Residue at 800°C (%)
PA6,6	391	438	1
PA6,6/CESA	366	415	2
PA6,6/ZrP	397	452	12
PA6,6/NS	338	452	5

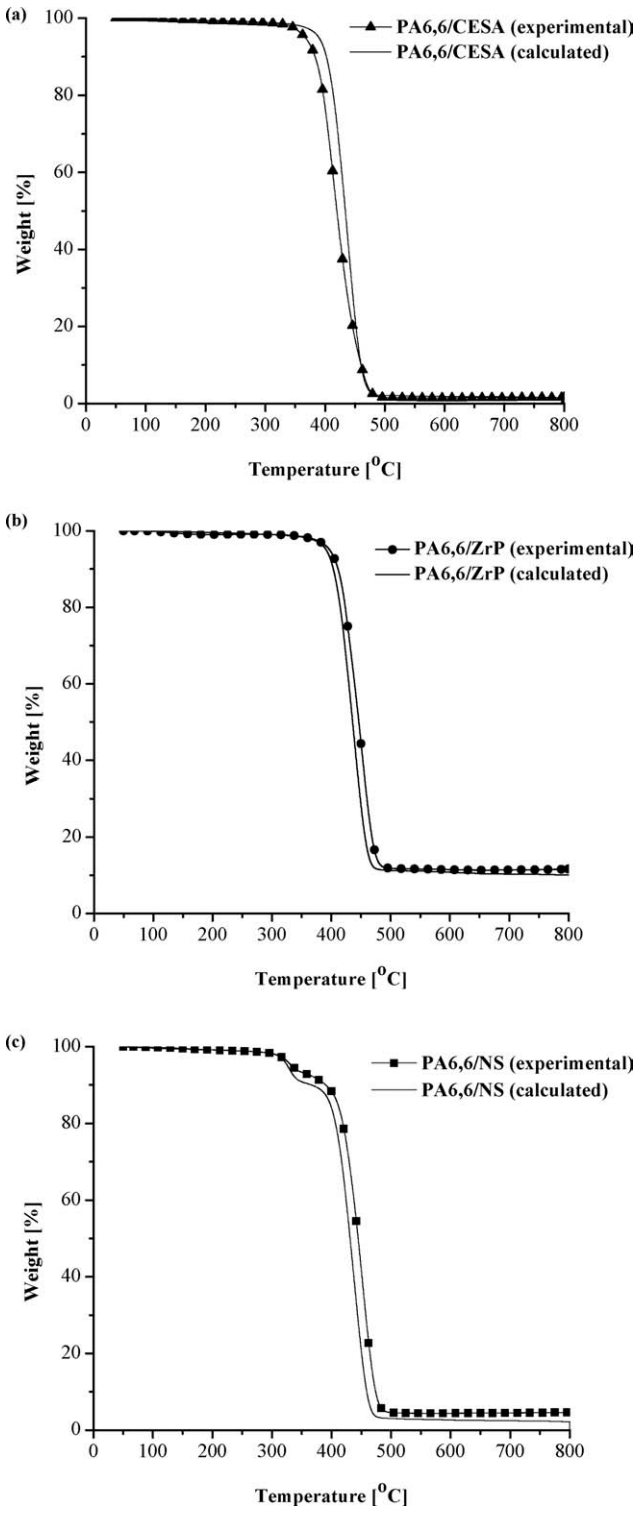

Figure 3 Experimental and calculated TG curves of the (a) PA6,6/CESA, (b) PA6,6/ZrP, and (c) PA66/NS composites.

nevertheless, T_{max} was the same as in the case of the PA6,6/ZrP composite.

To investigate the possible interactions between PA6,6 and additives during the degradation, the experimental TG curves were compared with the calculated ones. In the case of the PA6,6/CESA composite [Fig. 3(a)], when we compared the calculated curve with the experimental one, we observed that the latter was shifted to a lower temperature; this showed that the reactivity of PA6,6 with CESA led to thermal destabilization of the formulation.

In contrast, the experimental curves of the PA6,6/ZrP [Fig. 3(b)] and PA6,6/NS [Fig. 3(c)] composites shifted to higher temperatures compared with the calculated ones; we supposed that the degradation products of PA6,6 reacted with the degradation products of the additives and that this led to a thermal stabilization of the composites for temperatures higher than 376°C in the case of the PA6,6/ZrP composite and 406°C for the PA6,6/NS composite. Moreover, the amount of solid residue at 800°C (ca. 12 and 5 wt %, respectively, for the PA6,6/ZrP and PA6,6/NS composites) was slightly higher than was predicted from the independent decomposition of PA6,6 and the additive (ca. 10 and 2 wt %, respectively). These data evidenced that both additives promoted some charring of PA6,6.

Furthermore, the previously discussed findings were also evidence of the isothermal conditions, as shown in Figure 4. With the temperature at the beginning of the degradation of neat PA6,6 set at 390°C in a nitrogen atmosphere, the mass loss rate of the PA6,6/CESA composite was faster than that of neat PA6,6, whereas the both PA6,6/ZrP and PA6,6/NS composites showed the same loss mass rate in comparison with neat PA6,6 at the beginning; then, the mass loss slowed down, and this was clearly evident in the case of the PA6,6/ZrP composite.

Combustion behavior of the PA6,6 composite

The combustion behavior of the PA6,6 composites was investigated by means of cone calorimetry

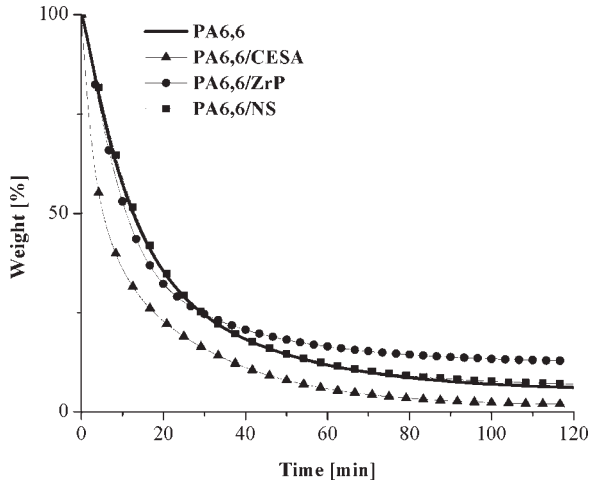

Figure 4 TG in isothermal conditions (390°C in a nitrogen atmosphere) of neat PA6,6, and the PA6,6 composites.

TABLE II
Cone Calorimeter Data of Neat PA6,6 and the PA6,6 Composites at 35 kW/m^2

Formulation	TTI ± σ (s)	PHRR ± σ (kW/m^2)	FIGRA ± σ (kW·m^{-2}·s^{-1})	TSR ± σ (m^2/m^2)
PA6,6	118 ± 15	1191 ± 163	5.24 ± 0.8	850 ± 21
PA6,6/CESA	84 ± 3	1032 ± 78	5.03 ± 0.8	1323 ± 6
PA6,6/ZrP	87 ± 13	734 ± 142	4.42 ± 1	674 ± 41
PA6,6/NS	60 ± 9	896 ± 13	5.15 ± 0.2	876 ± 99
PA6,6/C30B	99 ± 16	516 ± 32	2.63 ± 0.3	1404 ± 114
PA6,6/MBCNT	107 ± 2	554 ± 37	2.73 ± 0.3	1405 ± 107

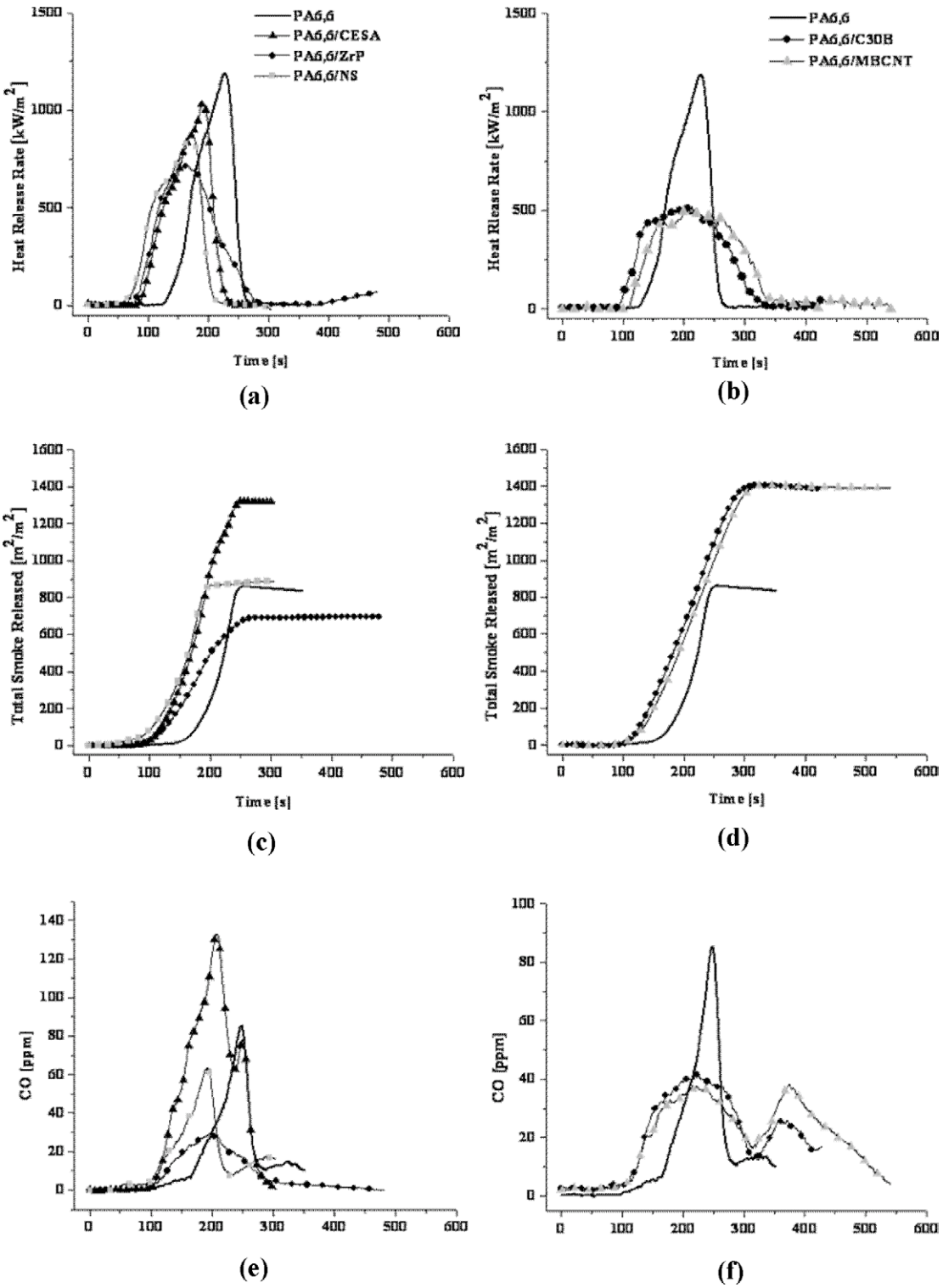

Figure 5 Curves of (a,b) HRR, (c,d) TSR, and (e,f) CO from the cone calorimetric tests.

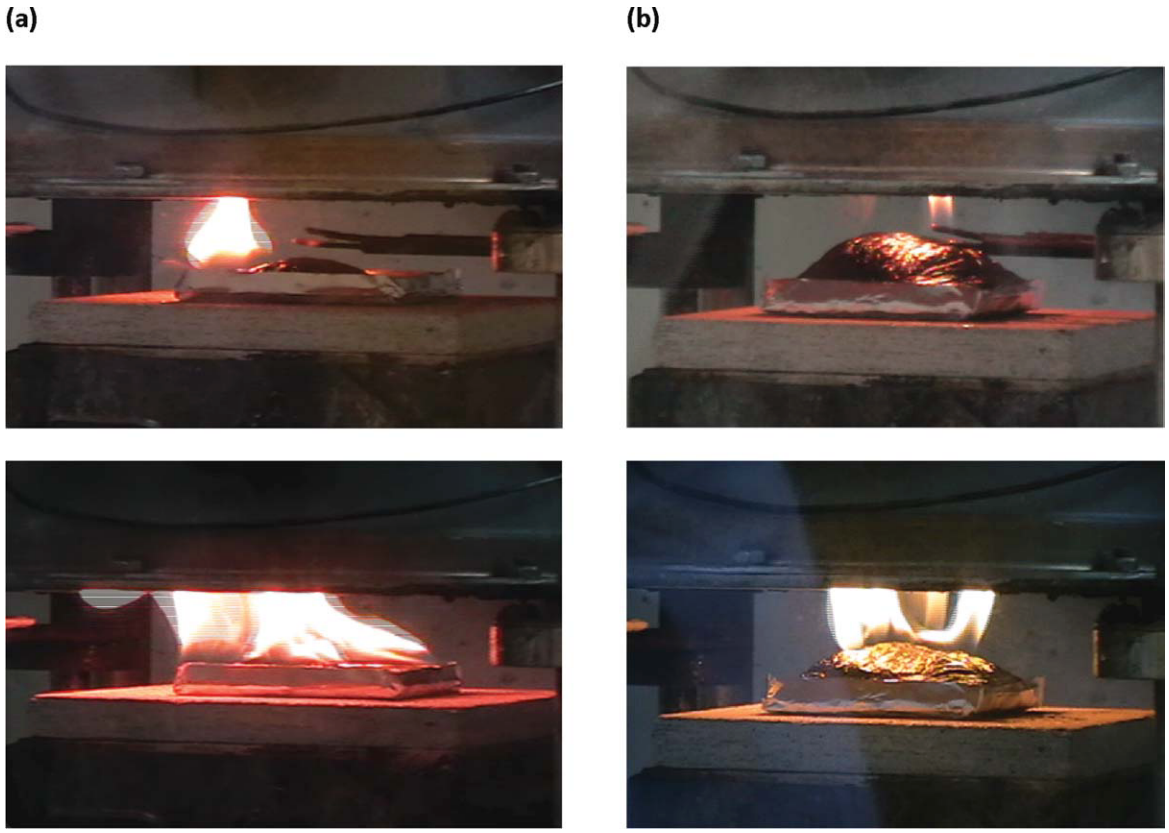

Figure 6 Digital pictures taken during the cone test (a) at TTI and (b) after ignition, 20 s later. [Color figure can be viewed in the online issue, which is available at wileyonlinelibrary.com.]

under a heat flux of 35 kW/m^2, and the fire-response parameters measured are reported in Table II and Figure 5(a–f).

Despite an earlier ignition of the novel PA6,6 composites (at 84, 87, and 60 s) compared to that of neat PA6,6 (at 118 s), the PA6,6/ZrP and PA6,6/NS materials exhibited a significant reduction of PHRR, with values of 38 and 25%, respectively [Fig. 5(a), Table II]. This result was much better than the one obtained with the halogen- and antimony-free flame retardant [PA6,6/CESA composite: −13% PHRR, Fig. 5(a), Table II]. Moreover, it can be said that the poor dispersion level of these novel additives within the PA6,6 matrix did not have a negative influence on this parameter, and further, it can be affirmed that one of the key factors of the decreased PHRR may have been the homogeneous distribution of the additive throughout the polymer matrix. Furthermore, the PA6,6/ZrP composite displayed the smallest value compared to neat PA6,6 and the PA6,6/CESA and PA6,6/NS composites in terms of FIGRA (Table II).

According to Segawa[31] and the references cited therein, ZrP has a lamellar structure, and each layer consists of planes of zirconium atoms bridged through phosphate groups, which alternate above and the below Zr atom planes. Between each layer, there are cavities filled with water of crystallization, which are stabilized by hydrogen bonding between phosphate groups. Each phosphate group in ZrP carries one ionizable hydroxyl group; this makes these materials highly acidic. Therefore, ZrP can act as a solid acid and, thus, catalyze the dehydrogenation of the polymer, which leads to the formation of carbon–carbon double bonds. At high temperatures, this can result in the generation of crosslinked or carbonized structures (char formation), according to Yang et al.[32]

Taking into consideration the previous description and the visual observation during the cone calorimeter test, we attributed the lower PHRR to the formation of expanded crust, which could act as a thermal insulator by slowing down the rate of thermooxidative degradation of the material exposed to heat. Moreover, we also supposed that the water from the lamellar structure of ZrP could participate in the dilution of combustible gases.

Our research group[20] previously showed the efficiency of NS in reducing the combustion rate of ethylene vinyl acetate copolymer due to the charring process and fuel dilution (the release of inert pyrolysis products, e.g., water vapor). In this study, as was also highlighted in the TG experiments, the same parameters may have been involved in decreasing the

TABLE III
LOI of the Neat PA6,6 and the PA6,6 Composites

Formulation	LOI (vol % O_2)
PA6,6	26
PA6,6/CESA	24
PA6,6/ZrP	24
Pa6,6/NS	25
PA6,6/C30B	23
PA6,6/MBCNT	24

combustion rate of the PA6,6/NS composite. On the other side, taking into consideration the visual observations during the cone calorimeter test [Fig. 6(a) vs 6(b)] and referring to the PA6,6/NS composite, we could explain the slowdown of the burning rate by the formation of an expanded crust; the same structure was not observed in the case of neat PA6,6 [Fig. 6(a)]. However, this expanded crust was not strong enough to prevent the fuel from feeding the flame or to hinder the diffusion of the oxygen to the specimen so the combustion was not finished until most of the fuel was burned out. In particular, Figure 6 shows digital pictures taken during the cone test at TTI [Fig. 6(a)] and after ignition [Fig. 6(b)], 20 s later.

The quantity and toxicity of the smoke (toxic gases, e.g., CO) released during the combustion, which is the primary cause of fatalities in most fires, are important parameters in terms of fire hazards (consequences of a fire). The PA6,6/CESA composite exhibited an increase of TSR of 56% compared to neat PA6,6, whereas the PA6,6/ZrP composite displayed a decrease of 21%. With regard to the PA6,6/NS composite, TSR was comparable with that of neat PA6,6 [Fig. 5(c)]. Furthermore, the evolution of CO as a function of time plotted in Figure 5(e) showed, once again, that the incorporation of ZrP into PA6,6 led to an improvement of the fire performance in comparison with neat PA6,6 and with the halogen- and antimony-free flame retardant. According to Levchik and Weil,[33] the smoke formation depends on the incomplete oxidation of the volatile products from the thermal degradation of polyamide. Therefore, the decrease of smoke production in the PA6,6/ZrP composite was probably caused by the catalytic effect of ZrP on the oxidation of the volatile products from the thermal degradation of PA6,6, as mentioned previously. This supposition was sustained in some way by Rocha et al.,[34] who studied the catalytic effect of ZrP on the cyclopentanone oxidation (with cyclopentanone being the major product of the degradation of PA6,6[2,22]).

Finally, Figure 5(b) shows the PHRR values of the PA6,6 composites based on conventional nanofillers (MBCNT and C30B).

A remarkable decrease of PHRR for both the PA6,6/MBCNT and PA6,6/C30B composites in comparison with neat PA6,6 was observed. The lower PHRR of the PA6,6/C30B composite could be explained by two mechanisms: one proposed by Gilman et al.[35] and showing that the degradation of the polymeric matrix containing clay produces a multilayered carbonaceous silicate structure that may act as an excellent insulator and also as a barrier to mass transport. The second mechanism was proposed by Zhu et al.[36] and demonstrated that the presence of iron in the clay can lead to some radical trapping reactions that will lower the heat release rate.

As far as the mechanism of carbon nanotubes as flame retardants are concerned, Kashiwagi et al.[37] reported that it could takes place through chemical or/and physical processes in the condensed phase. As far as we know, no work has been published reporting its influence on the fire retardancy of PA6,6. Even if the results show a strong decrease of PHRR (−53%) versus that of neat PA6,6, the PA6,6/MNCNT composite burned nearly completely. Furthermore, the reduction of PHRR was comparable to that seen with clay.

Although both the PA6,6/MBCNT and PA6,6/C30B composites showed an improvement in PHRR

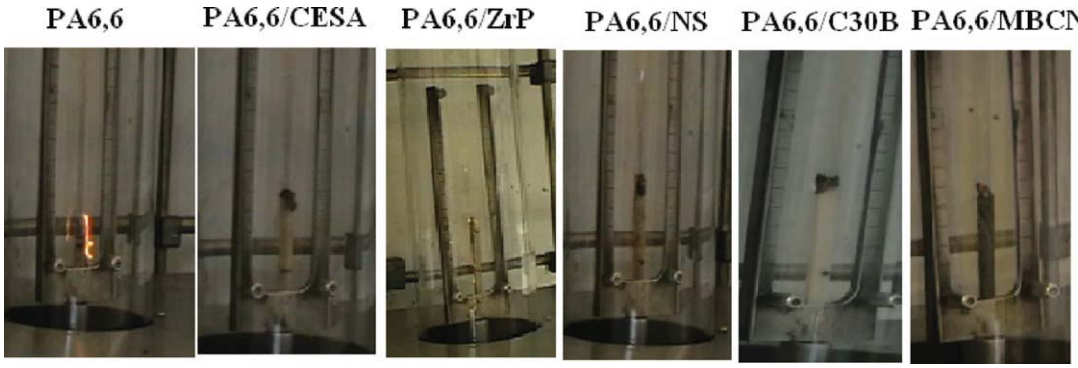

Figure 7 Digital photos taken at the end of the LOI test. [Color figure can be viewed in the online issue, which is available at wileyonlinelibrary.com.]

compared to that of neat PA6,6 and the novel PA6,6 composites, it can be underlined that with regard to the quantity of smoke [Fig. 5(d)], they showed a strong increase (TSR: +65% for both). The evolution of CO versus time is presented in Figure 5(f). This figure suggests that the incorporation of both types of conventional nanofiller into PA6,6 lowered the CO emissions.

Flammability study of the PA6,6 composites by LOI

LOI testing allows one to measure the minimum oxygen concentration needed for the self-sustained combustion of polymeric material (the LOI value is only expressed as a number). However, this test can also be used to analyze how the materials burn at oxygen concentrations corresponding to the LOI value.

The results obtained from LOI testing of the PA6,6 composites presented in Table III reveal that regardless of the additive type added to neat PA6,6, the LOI value of neat PA6,6 was slightly higher. Nevertheless, from visual observations, it was revealed that whereas neat PA6,6 melted with continuous dripping of the melt until the whole PA6,6 matrix was lost, all of the PA6,6 composites burned more slowly and not until the end because of the formation of a char/burn residue layer, which could act as a physical barrier against the propagation of the flame along the test specimen (Fig. 7, digital pictures taken at the end of the LOI test).

CONCLUSIONS

In this work, we found that the incorporation of ZrP and NS into PA6,6 enhanced the thermal stability of the polymer matrix at higher temperatures. Both additives significantly reduced the heat release rate of PA6,6. Furthermore, in the presence of ZrP, the quantity of smoke and CO emissions decreased considerably.

In contrast, the addition of CESA into PA6,6 decreased the thermal stability of PA6,6, as shown by T_{max}, whereas the flame retardancy, in terms of heat release rate, slightly decreased.

Concerning the PA6,6 composites based on conventional nanofiller (PA6,6/MBCNT and PA6,6/C30B), even when they showed the best results in terms of PHRR reduction, the quantity of smoke increased drastically.

Finally, a slight decrease in the oxygen concentration for ignition was seen with the addition of the additives mentioned previously to neat PA6,6. Nevertheless, the burning behavior of the PA6,6 composites at oxygen concentrations corresponding to the LOI value was quite different and showed no dripping tendency or burning at an extremely low rate compared to neat PA6,6, which melted and dripped until the whole neat PA6,6 was lost.

In the light of the aforementioned findings, we concluded that ZrP could be taken into consideration as a flame retardant for PA6,6.

The authors acknowledge the useful comments and suggestions of the reviewers.

References

1. Braun, U.; Schartel, B.; Firchera, M. A.; Jager, C. Polym Degrad Stab 2007, 921, 528.
2. Schartel, B.; Kunze, R.; Neubert, D. J Appl Polym Sci 2002, 83, 2060.
3. Gijsman, P.; Steenbakkers, R.; Furst, C.; Kersjes, J. Polym Degrad Stab 2002, 78, 219.
4. Liu, Y.; Wang, Q. Polym Degrad Stab 2006, 91, 3103.
5. Levchik, S. V.; Costa, L.; Camino, G. Polym Degrad Stab 1994, 43, 43.
6. Schartel, B.; Kunze, R.; Neubert, D. J Appl Polym Sci 2002, 83, 2060.
7. Levchik, S. V.; Levchik, G. F.; Murashko, E. A. Phosphorous-Containing Fire Retardans in Aliphatic Nylons ACS Symposium Series 787 (Fire and Polymers, Chapt.17, p 214); American Chemical Society: Washington, DC, 2001; p 214.
8. Qin, H.; Su, Q.; Zhang, S.; Zhao, B.; Yang, M. Polymer 2003, 44, 7533.
9. Song, L.; Hu, Y.; He, Q.; You, F. J Fire Sci 2008, 26, 475.
10. Williams, I. G. (to Imperial Chemical Industries). U.S. Pat. 4,548,977 (1985).
11. Williams, G. (to Imperial Chemical Industries). U.S. Pat. 4,552,912 (1985).
12. Scharf, D. J.; Ilardo, C. S.; Schwartz, W. T.; Salee, G. (to Occidental Chemical). U.S. Pat. 4,447,572 (1984).
13. Chang, E. P.; Ilardo, C. S.; Slagowki, E. L. (to Hooker Chemicals and Plastics Corp.). U.S. Pat. 4,194,072 (1980).
14. Ilardo, C. S.; Duffy, J. J. (to Occidental Chemical). U.S. Pat. 4,504,611 (1985).
15. Theysohn, R.; Penzien, K.; Seydl, W.; Wurmb, R.; Reimann, H.; Cordes, C. (to BASF Aktiengesellschaft). U.S. Pat. 4,137,212 (1979).
16. Lomakin, S. M.; Zaikov, G. E. New Concepts in Polymer Science. Ecological Aspects of Polymer Flame Retardancy; VSP: Utrecht, The Netherlands, 1999.
17. Dumler, R.; Lenoir, D.; Thoma, H.; Hutzinger, O. Chemosphere 1989, 19, 305.
18. Dumler, R.; Lenoir, D.; Thoma, H.; Hutzinger, O. Chemosphere 1990, 20, 1867.
19. Camino, G.; Costa, L.; Martinasso, G. Polym Degrad Stab 1989, 23, 359.
20. Alongi, J.; Poskovic, M.; Frache, A.; Trotta, F. Polym Degrad Stab 2010, 95, 2093.
21. Reaction-to-Fire Tests—Heat Release, Smoke Production and Mass Loss Rate—Part 1: Heat Release Rate (Cone Calorimeter Method); ISO 5660–1; ISP: Geneva, Switzerland, 2002.
22. Morgan, A. B.; Bundy, M. Fire Mater 2007, 31, 257.
23. Pielichowski, K.; Njuguna, J. Thermal Degradation of Polymeric Materials; Rapra Technology: Shropshire, United Kingdom, 2005.
24. Schaffer, M. A.; Marchildon, E. K.; Mcauley, K. B. J Macromol Sci Rev Macromol Chem Phys 2000, 40, 233.
25. Soto-Valdez, H.; Gramshaw, J. W. J Mater Sci Lett 2000, 19, 823.
26. Pack, S. P.; Clearfield, A. J Inorg Nucl Chem 1980, 42, 771.

27. Ferragina, C.; Di Rocco, R.; Fanizzi, A.; Giannoccaro, P.; Petrilli, L. J. Therm Anal Calorim 2004, 76, 871.
28. Thakkar, R.; Patel, H.; Chudasama, U. Bull Mater Sci 2007, 30, 205.
29. Genoveva, G. R.; Enrique, O. R.; Teresita, R. G. E.; Eduardo, O. R. Mineral Mater Char Eng 2007, 6, 39.
30. Trotta, F.; Zanetti, M.; Camino, C. Polym Degrad Stab 2000, 69, 373.
31. Segawa, K. Mater Chem Phys 1987, 17, 181.
32. Yang, D.; Hu, Y.; Song, L.; Nie, S.; He, S.; Cai, Y. Polym Degrad Stab 2008, 93, 2014.
33. Levchik, S. V.; Weil, E. D. Polym Int 2000, 49, 1033.
34. Rocha, G. M. S. R.; Santos, T. M.; Bispo, C. S. S. Catal Lett 2011, 141, 100.
35. Gilman, J. W.; Jackson, C. L.; Morgan, A. B.; Harris, R.; Manias, E., Jr.; Giannelis, E. P.; Wuthenow, M.; Hilton, D.; Phillips, S. H. Chem Mater 2000, 12, 1866.
36. Zhu, J.; Uhl, F. M.; Morgan, A. B.; Wilkie, C. A. Chem Mater 2001, 13, 4649.
37. Kashiwagi, T.; Grulke, E.; Hilding, J.; Groth, K.; Harris, R.; Butler, K.; Shields, J.; Kharchenko, S.; Douglas, J. Polymer 2004, 45, 4227.